Stomatal Closure, Basal Leaf Embolism, and Shedding Protect the Hydraulic Integrity of Grape Stems[1][OPEN]

Uri Hochberg*, Carel W. Windt, Alexandre Ponomarenko, Yong-Jiang Zhang, Jessica Gersony, Fulton E. Rockwell, and N. Michele Holbrook

Department of Organismic and Evolutionary Biology, Harvard University, Cambridge, Massachusetts 02138 (U.H., A.P., Y.-J.Z., J.G., F.E.R., N.M.H.); and Forschungszentrum Jülich, Institute for Bio- and Geosciences 2: Plant Sciences, 52425 Juelich, Germany (C.W.W.)

ORCID IDs: 0000-0002-7649-7004 (U.H.); 0000-0003-2400-5407 (C.W.W.).

The time scale of stomatal closure and xylem cavitation during plant dehydration, as well as the fate of embolized organs, are under debate, largely due to methodological limitations in the evaluation of embolism. While some argue that complete stomatal closure precedes the occurrence of embolism, others believe that the two are contemporaneous processes that are accompanied by daily xylem refilling. Here, we utilize an optical light transmission method to continuously monitor xylem cavitation in leaves of dehydrating grapevine (*Vitis vinifera*) in concert with stomatal conductance and stem and petiole hydraulic measurements. Magnetic resonance imaging was used to continuously monitor xylem cavitation and flow rates in the stem of an intact vine during 10 d of dehydration. The results showed that complete stomatal closure preceded the appearance of embolism in the leaves and the stem by several days. Basal leaves were more vulnerable to xylem embolism than apical leaves and, once embolized, were shed, thereby preventing further water loss and protecting the hydraulic integrity of younger leaves and the stem. As a result, embolism in the stem was minimal even when drought led to complete leaf shedding. These findings suggest that grapevine avoids xylem embolism rather than tolerates it.

Dehydration due to transpiration can place plants at risk of xylem cavitation, which results in a loss of conductance to water flow in the plant that, in the absence of regulation of transpiration, will ultimately drive leaf water potentials to catastrophic levels (Tyree and Sperry, 1988). However, plants do regulate transpiration by modulating stomatal aperture, the dominant resistance in the water transport pathway from the soil to the plant to the atmosphere (Van den Honert, 1948). The simplest phenomenological expectation is that plants adjust stomatal aperture to avoid xylem tensions that could trigger cavitation; accordingly, some researchers argue that significant stomatal closure precedes xylem cavitation (Cochard and Delzon, 2013; Hochberg et al., 2016b). Others believe that the two occur contemporaneously and hypothesize that embolism may play an important role in amplifying the hydraulic signal for timely stomatal closure (McCulloh and Meinzer, 2015; Trifilò et al., 2015; Klein et al., 2016). Note that the latter requires daily xylem refilling to restore the conductance of the embolized organs; but the only study that compared local xylem pressure and refilling showed that refilling will occur only under positive xylem pressure in grapevine (*Vitis vinifera*; Charrier et al., 2016). Understanding the time sequence of stomatal closure and cavitation during drought stress could resolve the extent to which plants can protect their hydraulic integrity.

One of the major challenges in unraveling these controversies is the difficulty of accurate evaluation of embolism (Cochard et al., 2013). Experimental artifacts (Choat et al., 2010; Wheeler et al., 2013; Pivovaroff et al., 2016) associated with the classic embolism evaluation protocols, such as the centrifuge technique (Pockman et al., 1995) or bench dehydration (Sperry et al., 1988), can sometimes result in overestimation of the degree of embolism in some species. Moreover, most methods to estimate embolism require the destruction of the evaluated organs; therefore, continuous monitoring is not possible. For that reason, previous publications that address the interaction between stomatal conductance (g_s) and embolism either compare averages from a limited number of time points during the experimental

[1] This work was supported by a Vaadia Binational Agricultural Research and Development Fund postdoctoral fellowship (grant no. FI-522-2015 to U.H.), the Materials Research Science and Engineering Center at Harvard University (grant no. DMR 14-20570 to A.P.), the National Science Foundation (grant no. IOS 1456836 to F.E.R.), and the Air Force Office of Sponsored Research (grant no. FA9550-09-1-0188 to N.M.H.).

* Address correspondence to uriho9842@yahoo.com.

The author responsible for distribution of materials integral to the findings presented in this article in accordance with the policy described in the Instructions for Authors (www.plantphysiol.org) is: Uri Hochberg (uriho9842@yahoo.com).

U.H. conceived the experiment with F.E.R. and N.M.H. and executed the measurements of growth, gas exchange, and imaging with A.P. and J.G.; Y.-J.Z. performed the hydraulic measurements; C.W.W. performed the MRI experiment; the article was written by U.H. with major contributions by all authors.

[OPEN] Articles can be viewed without a subscription.

www.plantphysiol.org/cgi/doi/10.1104/pp.16.01816

period (Zufferey et al., 2011) or integrate the response functions of embolism and g_s to xylem pressure (Brodribb et al., 2003). In the first approach, experimental variability overcasts the temporal rhythm, while in the second, overlap in the water potential domain (based on equilibrium measurements as in the pressure chamber or psychrometer) does not necessarily imply overlap in the time domain (Rockwell et al., 2014a).

Visualization techniques such as microcomputed tomography (microCT) and magnetic resonance imaging (MRI) provide reliable measurements of xylem embolism in intact plants (Scheenen et al., 2007; Cochard et al., 2015) and even embolism propagation over time in the same plant (Holbrook et al., 2001; Brodersen et al., 2010, 2013; Choat et al., 2015; Hochberg et al., 2016a). However, these approaches also have drawbacks: small field of view, long acquisition times, potentially lethal radiation doses for the imaged plant (in the case of microCT), expense, and limited availability of the equipment. Therefore, there is a need to develop reliable, affordable, and accessible methods to evaluate embolism in intact plants. Recently, Brodribb et al. (2016b) introduced an optical method to observe embolism spread through the leaves of intact plants that meets all of the aforementioned criteria. Here, we utilized this method to continuously monitor embolism formation in the leaves of dehydrating grapevine while simultaneously measuring g_s, with the goal of resolving their temporal sequence. As the method enabled us to explore embolism in intact plants, we followed the plants' performance after rehydration to determine the fate of embolized leaves. Additionally, embolism of stems and leaves from different nodal positions (older basal versus younger apical leaves) was monitored to characterize the plant-level strategy for maintaining hydraulic integrity.

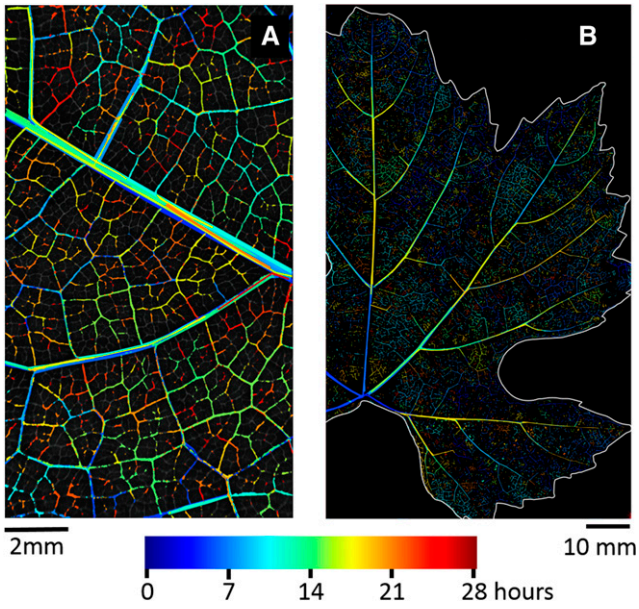

Figure 1. Embolism spread in a leaf imaged with a microscope (A) or a scanner (B). The largest vein visible in the microscope image (A) is the midrib. Cavitation events are colored according to their time of occurrence. Early cavitation events in the major veins are overlaid with later cavitation events. The full time course of embolism propagation can be observed in Supplemental Movies S1 and S2.

RESULTS

Experiment 1: Dehydration by Cutting the Root-Stem Junction

The new optical technique (Brodribb et al., 2016b) allowed us to follow the temporal and spatial propagation of embolism in grapevine leaves. The dynamics of embolism propagation highlight the spatial patchiness of the process, in which neighboring vessels tend to cavitate in temporal proximity (Fig. 1; Supplemental Movies S1 and S2).

The results from the first experiment, in which water deficits were induced by severing shoots at the root-stem junction, showed a large temporal separation between stomatal closure and embolism appearance in the leaf (Fig. 2). Immediately after severing the vine, g_s increased by 30% to 60%, probably as a result of decreased epidermal turgor (i.e. wrong-way response or Iwanoff effect; Mott and Franks, 2001). However, following this initial increase, g_s fell exponentially, reaching 20% of its initial value (from 60–130 mmol m^{-2} s^{-1} down to values of 12–22 mmol m^{-2} s^{-1}) after 1.7 ± 0.4 h (n = 4). In contrast, it took 5.3 ± 1.2 h from the cutting of the vine to develop 1% embolism. At that time (of 1% embolism), g_s was 1% to 6% of its initial (precut) value, with absolute g_s values of 2 to 6 mmol m^{-2} s^{-1} (Fig. 2), which are similar to published estimates of cuticular conductance (Boyer et al., 1997), suggesting that the stomata were fully closed. Measurements of leaf water potential (Ψ_l) in the drying vines using a pressure chamber showed that 1% embolism occurred when Ψ_l ranged from −1.39 to −1.56 MPa. Wilting occurred primarily in the first 2 h after the shoot was cut and at least 2 h before 1% embolism (Figs. 2 and 3).

It is important to mention that, in two plants, early cavitation in a single xylem element did occur. In one of them, cavitation was observed 12 min after cutting the vine at the base of the stem, when g_s was declining back to the original values following the wrong-way response. In the second vine, a single event was observed 45 min after the vine was severed, when g_s was at 33% of its initial value. In both cases, additional cavitation was not observed for several hours. Because the embolized conduits in these two instances were only 1.2 and 2.7 mm long and ~20 μm in diameter (size estimations are based on the changes in light transmission), their contribution to conductance was negligible. A summary of the results from this first experiment is presented as a short movie at https://www.youtube.com/watch?v=7-X8mmPFek0.

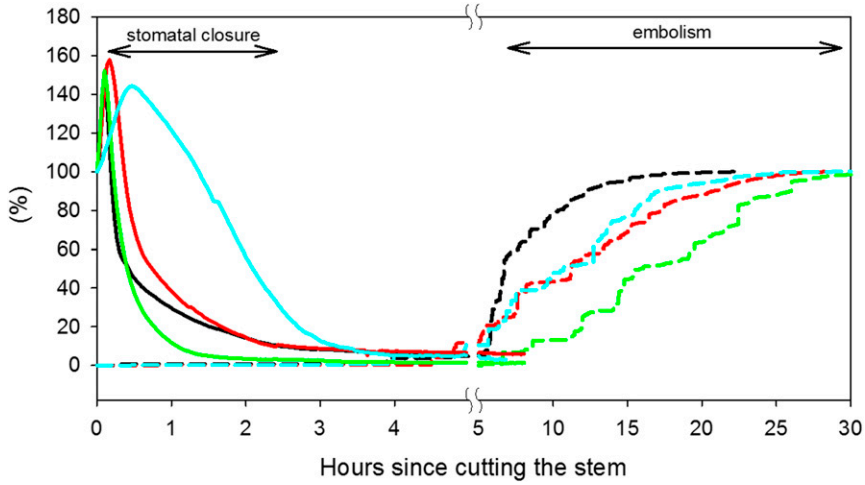

Figure 2. The g_s (percentage of maximal values; solid lines) and embolism (dashed lines) in four dehydrating grapevines (experiment 1) as a function of time since cutting. The different colors represent the four repetitions.

Experiment 2: Dehydration of Intact Plants

Withholding water from intact plants resulted in a similar temporal pattern: plants reached nearly minimal g_s (14.2% of initial value) on average 3 d before the appearance of xylem embolism (Fig. 4). When xylem embolism was detected, leaves had already wilted and g_s was less than 10% of the original values, with an average absolute value of 5.4 mmol m^{-2} s^{-1}. Analysis of the data from both experiments showed that, for plants that are disconnected from their roots (as in experiment 1) and also for intact plants (as in experiment 2), a reduction of g_s to nearly minimal levels occurred at –1.1 MPa and the appearance of leaf embolism occurred at values lower than –1.4 MPa (Fig. 5). In the second experiment, because embolism and water potential were evaluated once per day, it was not possible to determine the exact value at which embolism appeared. However, the range in which the first appearance was detected ($-1.46 < \Psi_l < -1.75$ MPa; based on average Ψ_l values of embolism day and the previous day) matched the values that led to embolism in the first experiment (Fig. 5).

Within 25 h after the first sign of xylem embolism, the plants were rewatered. All leaves regained turgor within 12 h of irrigation, but in the following week, over 50% of the leaves were shed or showed signs of senescence (necrosis and yellowing; Fig. 4). Leaves that were not impaired by the dehydration restored their g_s to prestress values 5 d after the rehydration. Most of the shed leaves were basal (nodal position index < 0.5; Fig. 6), raising the question of whether there were differences in vulnerability to cavitation between basal and apical leaves.

We tested the difference in vulnerability to cavitation due to nodal position by comparing basal and apical leaves on the day that embolism was detected in a leaf from the middle of the shoot. Leaves were measured with both a modified optical method (see "Materials and Methods") and a standard percentage loss of conductance (PLC) measurement. The measurement revealed that gray levels were modified by an average of 5.2% in the basal leaves but only by 0.6% in the apical leaves, suggesting more embolism in the basal leaves. This difference agreed well with the petiole hydraulic measurements, showing that the PLC of petioles from basal leaves was 64%, compared with 39% in the petiole of the apical leaves and 14% in petioles of the control vines. Perhaps more striking than comparing the average difference is that, when comparing leaves from the same shoot, the basal one always showed a significantly higher degree of embolism (either through gray level ratio or PLC) than its respective apical one ($P < 0.005$, paired-samples Student's t test). Interestingly, and in

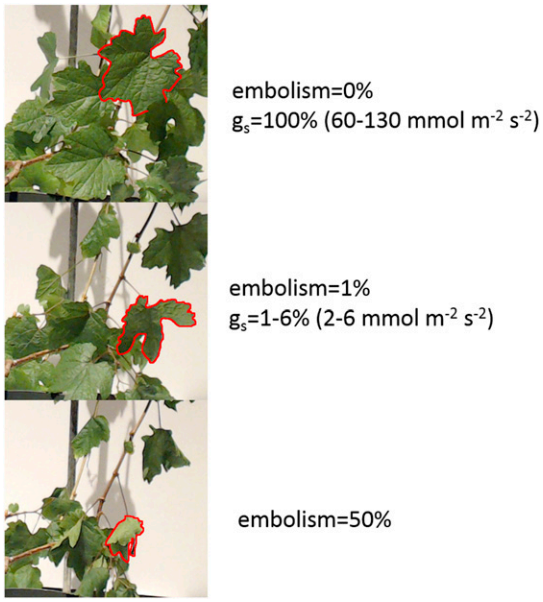

Figure 3. Images of a dehydrating plant at 0%, 1%, and 50% embolism. The 0% embolism image was taken prior to cutting the vine. The range of g_s values of the four plants at 0% and 1% embolism is presented. To facilitate the observation of leaf appearance at different stages, the same leaf is outlined in red in all three images.

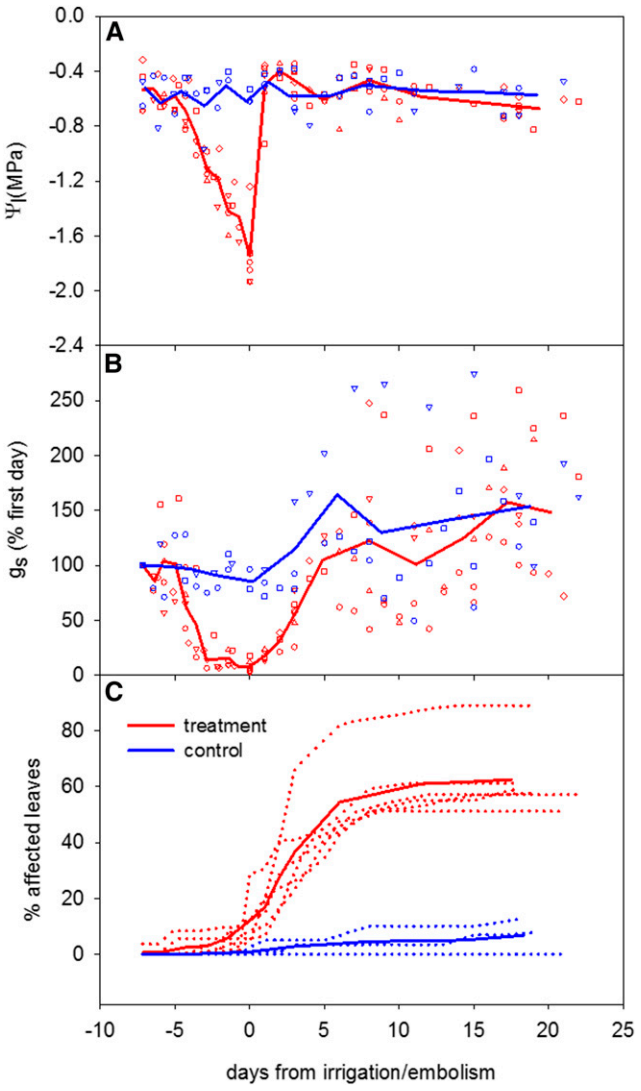

Figure 4. Ψ_l (A), g_s (B), and the percentage of affected leaves (C) as a function of days from first detection of embolism in treatment (red) and control (blue) plants. Affected leaves account for yellow, necrotic, or shed leaves. Plants were dehydrated until embolism was detected (day 0) and then irrigated daily for another 20 d. The open symbols (in A and B) or dots (in C) represent six replicate plants (each with a different symbol). The thick lines represent the averages for each treatment (n = 6). The response times of each replicate before irrigation/embolism (negative values) are scaled to the average number of days between the initiation of dehydration and the embolism appearance (7.16 d; see "Materials and Methods"), whereas positive values are actual days.

accordance with the hydraulic segmentation known in grapevine (Charrier et al., 2016; Hochberg et al., 2016a), the stems of dehydrated grapevine showed only 7% PLC, close to the average value of control plants (Fig. 7).

Experiment 3: MRI Dehydration

To confirm our finding that leaf shedding occurred without a significant level of stem embolism, we repeated the pot dehydration experiment with one grapevine while stem embolism was evaluated in the intact plant using MRI (Fig. 8). Wilting occurred 1 week after irrigation was withheld, but it took an additional 3 d to reach 5.9% or 4.1% stem PLC (estimates based on Hagen-Poiseuille calculations from xylem vessel diameter or MRI volume flow maps; Fig. 8). At that time (10 d after the last irrigation), the plant was rehydrated, but only four out of 80 leaves regained turgor, and even these quickly turned yellow and were shed (three of these within 1 d after rehydration). Figure 8D shows the appearance of the plant that was dried in the MRI to a mild stem embolism (less than 10%) 3 d after rehydration. A volume flow map (Fig. 8B) showed that large volumetric flow coincides with large diameter vessels and that all large vessels were conductive, including those in the outer periphery of the stem, suggesting that the calculation of PLC from MRI or microCT analysis based on the Hagen-Poiseuille equation is a reliable approach. It is important to note that, because MRI has a minimal flow detection threshold, it is not possible to determine whether the narrowest classes of vessels were conductive.

DISCUSSION

To our knowledge, our results provide the first in vivo measurements of embolism formation in grapevine leaves in concert with g_s and stem and petiole hydraulic measurements. A finding of particular interest is that, at Ψ_l between −1.1 and −1.4 MPa, stomata were completely closed while cavitation was not yet observed. This observation challenges evidence for the contemporaneous appearance of embolism and stomatal down-regulation (Zufferey et al., 2011) or the hypothesis that the induction of embolism could act as a signal for stomatal closure (Nardini and Salleo, 2000). While the Ψ_l required for almost complete stomatal closure (−1.1 MPa) or for embolism induction (−1.4 MPa) was similar in both experiments, the time difference between these processes was extended from 4 h in dehydration of excised shoots up to 4 d in pot dehydration and is expected to be even longer for plants with larger root volume. Only under prolonged drought conditions, when the plant has depleted the soil water reservoir, would the critical Ψ_l leading to a significant number of leaf cavitation events be expected. Our experimental approach showed that processes occurring in a small interval of Ψ_l could be well separated in time, as in the clear temporal separation between stomatal closure and embolism appearance.

Our findings show that a Ψ_l low enough to induce leaf embolism also leads to massive leaf shedding, supporting the idea that grapevine employs an embolism avoidance strategy (rather than tolerance) and obviates the need for leaf xylem refilling. In agreement, leaf senescence in many other species was associated with a decline in hydraulic conductivity (Brodribb and Holbrook, 2003; Wolfe et al., 2016), and while it is hard

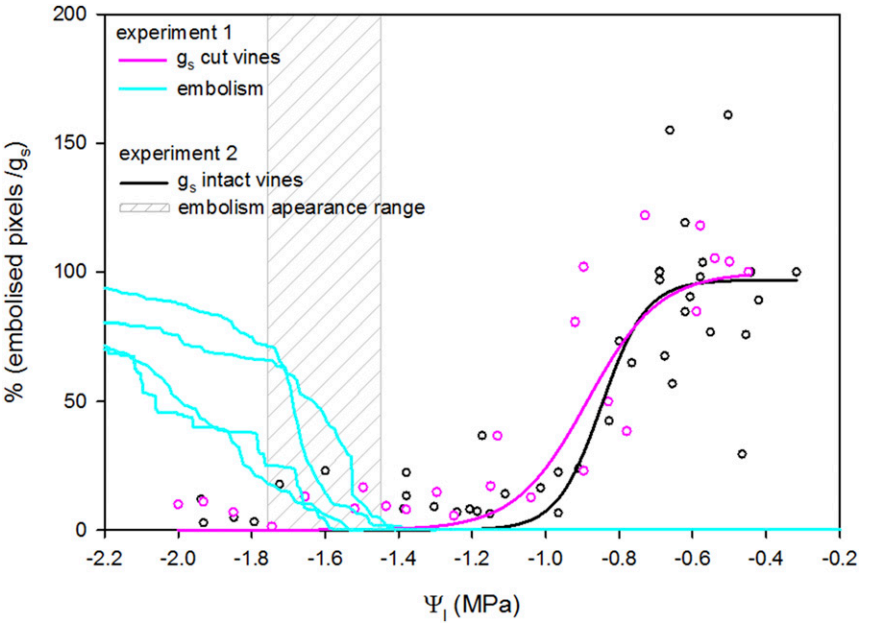

Figure 5. Similar responses of g_s (pink and black) and embolism (cyan and gray) to Ψ_l in both experiments. The data are a combination of experiment 1 (cut vines; pink for g_s and cyan for embolism) and experiment 2 (intact vines; black for g_s and gray for embolism). In experiment 2, because embolism and water potential were evaluated once per day, it was difficult to determine the exact water potential value that led to embolism: the likely range is indicated by the gray area, which is bounded by the average Ψ_l taken on the day before and the day of embolism detection.

to determine whether there are causal links between leaf embolism and shedding, or if they are simply coordinated through leaf water status, it appears that a leaf with a higher degree of embolism (those located near the base of a shoot) has a higher chance of being shed. Because grapevine basal leaves tend to have higher (closer to zero) Ψ_l than apical leaves (Schultz and Matthews, 1988; Lovisolo and Schubert, 1998), their high degree of embolism relative to apical leaves (Fig. 7) probably is not a function of Ψ_l differences but rather of differences in vulnerability to embolism among leaves at different positions. The higher vulnerability of basal leaves might originate from their older age and subsequent enhanced development, characterized by higher connectivity, and the increased abundance of air seeding sources compared with apical leaves. With regard to higher connectivity, Chatelet et al. (2006) showed for cv Chardonnay vines that xylem vessel length in basal leaves is longer than in apical ones, characterized by a direct connection (i.e. no intervessel pit membranes) between two of the most vulnerable places in the xylem: the leaf major veins (Fig. 1) and the stem primary xylem (Fig. 8; Brodersen et al., 2013). This increased connectivity in basal leaves likely facilitates embolism

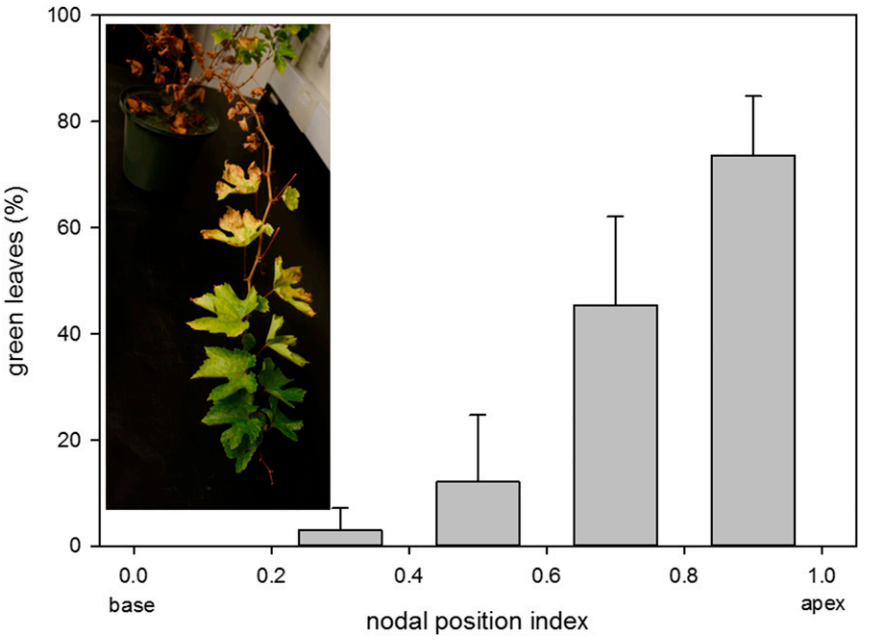

Figure 6. Percentage of green leaves as a function of nodal position index (node number/total nodes on the shoot) 20 d after rehydration. Leaves from the base of the shoot have much lower chances for survival after a critical water stress compared with leaves located near the shoot apex. Data are averages ± SE; $n = 6$. The inset shows a branch at the end of the experiment illustrating the spatial gradient of leaf shedding.

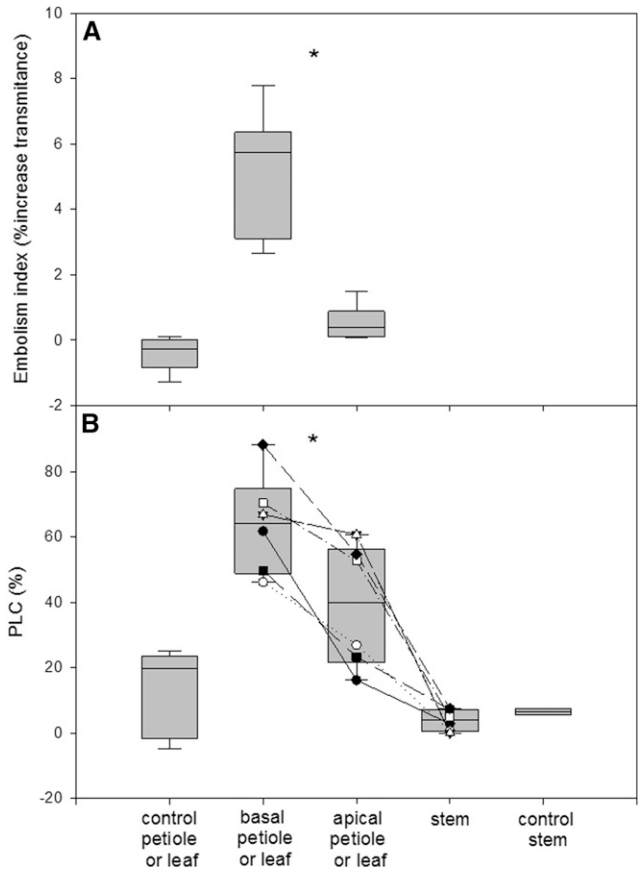

Figure 7. Higher degree of cavitation in leaves of low nodal position (close to the shoot base). The degree of embolism was compared using two different methods: the change in the veins' gray values from before to after pressurizing the leaf with water (20 mmol of KCl) at 150 kPa for 3 min (A) and the PLC (B). The stems and petioles of high and low nodal position were taken from drying plants when embolism was observed. Control petioles and control stems were taken from well-watered plants. The boxes represent the 25th and 75th percentiles, and error bars indicate SD. In B, similar symbols connected by lines are measurements of petioles or stems from the same shoot, presented to better emphasize the difference between tissues. Asterisks represent significant differences (*, $P < 0.005$) between petioles from high nodes (average nodal position index was 0.77) and petioles of lower nodes (average nodal position index was 0.34). Data were compared using paired-samples Student's *t* test; $n = 8$ and $n = 6$ for A and B, respectively.

propagation. With regard to the increased abundance of air seeding sources, basal leaves contain more protoxylem lacunae (i.e. a lower proportion of water-filled protoxylem) compared with elongating organs, such as apical leaves or stems. These lacunae are a probable source for gas propagation into the xylem network through shared pits between metaxylem and protoxylem (Lens et al., 2013; Rockwell et al., 2014b). A higher lacuna abundance, combined with increased connectivity, could explain the increased vulnerability of basal regions compared with apical parts (Fig. 7; Charrier et al., 2016), leading to functional protection of young, productive leaves over older ones.

The significant difference in embolism degree between basal leaves, apical leaves, and the stem (Fig. 7) agrees well with the plant segmentation hypothesis (Zimmermann, 1983) and adds a new perspective to it in terms of segmentation among leaves from different nodal positions. According to the segmentation hypothesis, plants sacrifice organs of lesser importance and investment to save organs that are critical for long-term survival and propagation (Zimmermann, 1983). Such segmentation is supported in grapevine by the finding that petioles and roots are more vulnerable to cavitation than stems (Lovisolo et al., 2008; Charrier et al., 2016; Cuneo et al., 2016; Hochberg et al., 2016a). Combining these previous findings with our observation that, on average, the midrib cavitates before higher vein orders (for clear visualization, see Supplemental Fig. S1; Supplemental Movies S1 and S2) points toward the midrib or petiole as the most vulnerable section of the xylem sap pathway in grapevine. Similar observations in several other species using microCT (Scoffoni et al., 2017) or the optical technique (Brodribb et al., 2016a) suggest that high xylem vulnerability of the midrib/petiole is shared by many plants. In agreement, Cochard et al. (2002) found that the leaf rachis in walnut

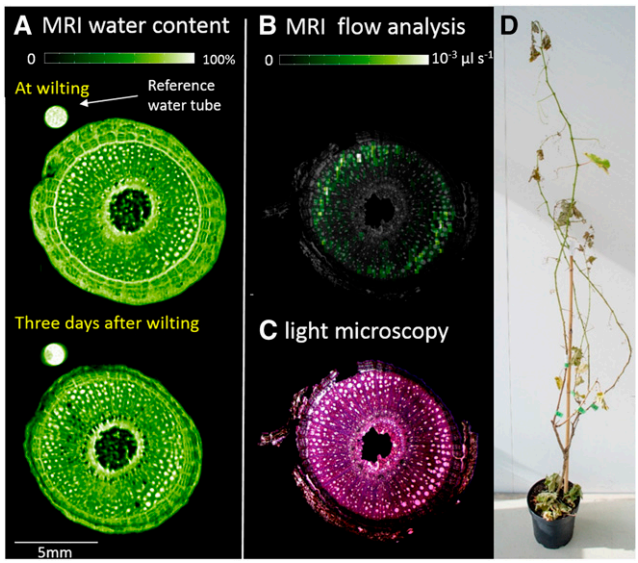

Figure 8. A plant that was dried for 10 d to less than 10% stem embolism while being imaged continuously using an MRI scanner. A, In the MRI water content image, bright pixels represent a high water content (as appears in the reference tube or in sap-filled xylem vessels) and black pixels represent the absence of water (as appears in the pith or in gas-filled xylem vessels). B, In the volume flow map, bright pixels represent a high flow rate and dark pixels represent a low flow rate. C, The PLC was evaluated to be 5.9% based on Hagen-Poiseuille calculation from vessel diameters, as measured in the light microscopy cross section, as opposed to 4.1%, based on the conductance value of the embolized pixel taken from the MRI volume flow map in B. D, This photograph was taken 3 d after the plant was rewatered, showing that drying a vine to a mild degree of stem embolism (less than 10%) results in the shedding of all its leaves.

(*Juglans regia* × *nigra*) was significantly more vulnerable to cavitation than the stem and slightly more vulnerable than the midrib, describing it as the Achilles heel of the xylem sap pathway. From a functional perspective, the high xylem vulnerability of these organs renders them hydraulic fuses (Zufferey et al., 2011; Wolfe et al., 2016): in the case that stomatal regulation fails to maintain Ψ above the cavitation threshold, embolism in the petiole and veins of basal leaves, followed by leaf shedding, will prevent further water loss and protect the hydraulic integrity of younger leaves and the stem.

Our findings suggest that the occurrence of stem embolism in commercial vineyards is probably rare. The literature, however, contains many studies showing potted grapevine with significant embolism in their stems. These experiments were designed to quickly generate high xylem tension to test the physical interaction between Ψ and cavitation but not necessarily to simulate natural dehydration. For example, Brodersen et al. (2013) used 0.7-L pots, allowing for very fast dehydration, possibly shorter than the time frame required for biological responses (e.g. ethylene production and the activation of abscission zone cells). In a vineyard, stomatal closure should prevent the soil from drying, and even if it failed to do so, vulnerable basal leaves would be embolized and shed many days before their cuticular conductance could drive the soil to a Ψ that is predicted to cause significant xylem embolism in the stem. For example, when Schultz (2003) stopped irrigation in a cv Chardonnay vineyard (with less than 50 mm seasonal precipitation), it took 3 months to reach a Ψ_l of −1.8 MPa, and at the end of that period, the vines had less than half of the leaf area of the irrigated controls. If all lines of defense are breached and the stem is significantly cavitated, assuming rehydration will take place when the plant is still alive, root pressure combined with the absence of leaves should lead to positive pressures for a sufficient time to refill the xylem in the stem, such that it may again sustain negative pressures and allow the emergence of new buds (Knipfer et al., 2015; Charrier et al., 2016).

Because most cavitation occurred at Ψ lower than −1.5 MPa, long after the leaves had wilted, it is likely that grapevine is less vulnerable to cavitation than some researchers have argued. For example, Jacobsen et al. (2015) present a summary of findings that support 50% loss of conductivity due to embolism in grapevine stems under Ψ ranging from −0.16 to −0.76 MPa. Such Ψ levels are typical of well-irrigated vines with high rates of g_s and without any sign of wilting (Herrera et al., 2015; Hochberg et al., 2017). Based on our data from hydraulic measurements, the optical method, and MRI analysis, it seems unlikely that those water potentials will lead to embolism. In support, microCT visualization of grape showed very few embolized vessels at Ψ > −1 MPa (Brodersen et al., 2013; Charrier

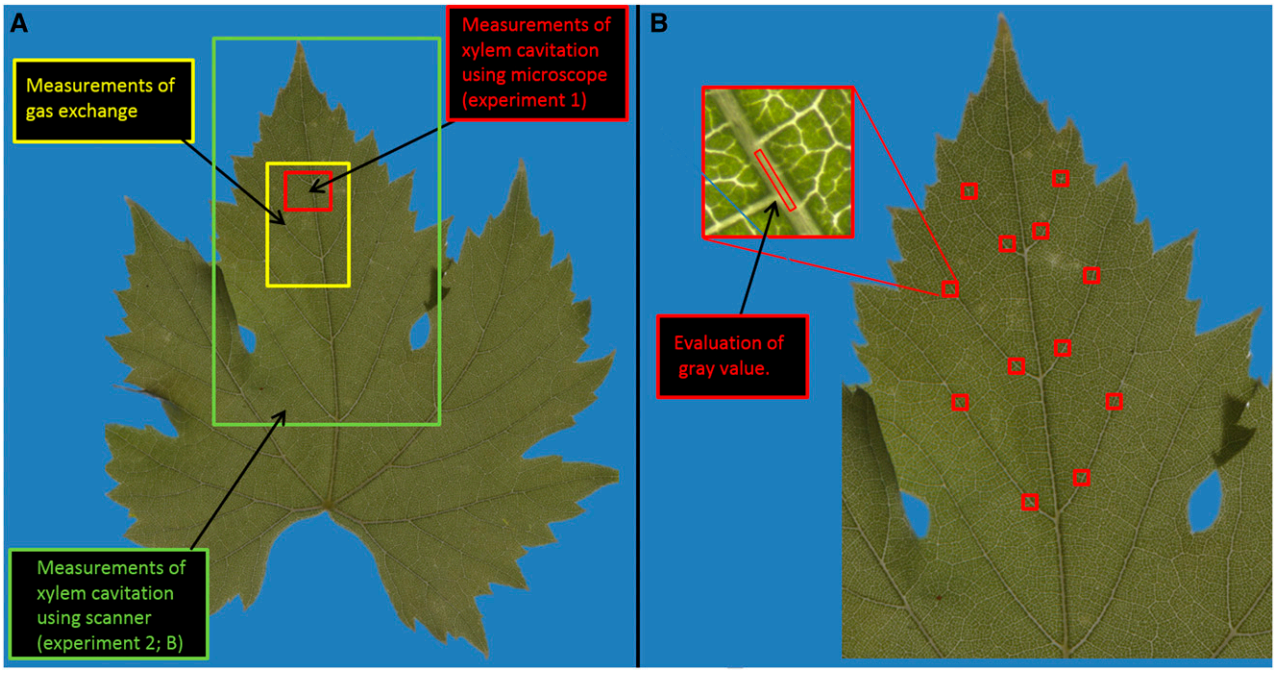

Figure 9. Leaf areas that were used in the different experiments. A, In experiment 1, the red area (1 × 1.7 cm) was imaged using a microscope for embolism detection and the yellow area (2 × 3 cm) was used for gas exchange. Note that measurements of gas exchange and xylem cavitation were carried out on separate leaves attached to the same plant. B, In experiment 2, the green area was imaged using a scanner (the entire area shown). To evaluate the amount of embolism in leaves that were not followed during dehydration, we selected 12 points (red squares) located on second order veins. Gray values of small polygons (~150 pixels; 30 × 500 μm^2) from the center of the vein were measured before and after flushing the leaf with water at 150 kPa.

et al., 2016; Hochberg et al., 2016a). Jacobsen et al. (2015) argue that imaging techniques (microCT and MRI) underestimate the degree of embolism, since they account also for young and nonconducting vessels on the outer periphery of the stem, leading to overestimation of maximal conductance and underestimation of PLC. Our flow measurements (Fig. 8B), however, demonstrate that there are only a few nonconductive vessels and that they could not possibly be the source of the difference between imaging techniques and the values presented by Jacobsen et al. (2015). In fact, it appears that the small xylem vessels near the pith (possibly primary xylem) are nonconductive. Because these vessels are the first to cavitate (Fig. 8; Brodersen et al., 2013), their incorporation into the calculation of PLC would actually overestimate the degree of embolism rather than lead to an underestimation of it. Both PLC calculations based on the diameters of all vessels or the MRI volume flow map resulted in a low embolism degree (5.9% or 4.1%, respectively). The apparent contradiction between some previous publications (Jacobsen et al., 2015) and our findings could have resulted from the overestimation of native embolism in grapevine when using both the bench dehydration and centrifuge techniques (McElrone et al., 2012; Hochberg et al., 2016b). Because many other long-vesseled species were shown to be sensitive to the same artifacts (Wheeler et al., 2013; Torres-Ruiz et al., 2014, 2015; Pivovaroff et al., 2016), we believe that the new optical method, which is not subject to these artifacts, provides an excellent tool to answer some of the controversies regarding plant susceptibility to embolism.

One of the most striking features of grape leaf cavitation is the patchiness of the process (Supplemental Movies S1 and S2), which, in turn, provides strong support for the air seeding hypothesis (Zimmermann 1983). Discrete areas of the leaf tend to cavitate together, while other areas remain water filled under substantially higher tensions. This finding could imply that vessels in the same area of the leaf have similar vulnerability to cavitation or, more probably, that most vessels are not tested before gas is present in a neighbor with which they share pit connections. Combining the wide range of xylem vulnerability shown by single vessel air injection (Christman et al., 2012; Venturas et al., 2016) and our observation that vessels tend to cavitate mostly after their neighboring vessels are embolized suggests that the patchiness phenomenon is caused by highly resistant vessels that, once embolized, expose a whole region of less resistant conduits to gas. In accordance with the aforementioned vulnerability segmentation, it would make sense that these highly resistant vessels are located in hydraulically critical positions. For example, resilient xylem areas such as the leaf minor veins (Fig. 1) could be separated from the more vulnerable major veins by highly resistant pits. As vessels in major veins are in embolism danger due to connection with protoxylem lacunae (unlike minor veins; Zhang et al., 2016), reinforcing pits in critical junctions between the major and minor veins would be an inexpensive way to prevent embolism propagation throughout the xylem network.

From a methodological standpoint, our findings support the validity of embolism evaluation techniques. When using the bench dehydration technique to generate tension, the exposure of vessels to air raised concerns that gas could propagate from the cutting point, through vulnerable pits, to the organ under evaluation. The similar Ψ_l (−1.5 MPa) that led to cavitation in the leaves of detached or intact plants (Fig. 5) suggests that the drying procedure does not affect the leaf xylem vulnerability. It appears that, even when air is introduced into the shoot by cutting, it does not propagate into the leaf if the stems are long enough, providing important evidence that studying leaf xylem vulnerability with the bench dehydration method is a reliable approach. In addition, the findings of the reversed optical method (Fig. 7A) reinforce the validity of embolism detection through light transmission. The increase in light transmission generated by xylem refilling when leaves were pressurized with water at 150 kPa (Fig. 7A) suggests that the decrease in light transmission during dehydration indeed originates from xylem cavitation.

To conclude, our results unfold the temporal sequence of different physiological responses to dehydration. Stomatal regulation is the first safety mechanism activated to avoid the leaf cavitation threshold. If that critical Ψ_l is reached despite the down-regulation of g_s to minimal values (i.e. cuticular conductance), embolism and shedding of basal leaves further reduce water loss, thereby protecting the hydraulic integrity of the apical leaves and the stem. While it can be difficult to resolve differences in threshold Ψ_l for these processes, their separation in time will scale with the size of the soil water reservoir, which is many days under field conditions, highlighting the importance of a temporal perspective for understanding plant embolism avoidance strategies.

MATERIALS AND METHODS

Three experiments were performed in this study. The first two were performed at Harvard University and the third at the Forschungszentrum Jülich. In experiment 1, we studied embolism propagation in leaves of grapevine (*Vitis vinifera*) plants that were disconnected from their roots while simultaneously measuring their g_s, in an attempt to resolve their temporal sequence. In experiment 2, we tried to validate the findings from experiment 1 in intact plants and also understand the fate of leaves experiencing a mild degree of embolism. For that purpose, we withheld irrigation from potted grapevine until the first sign of xylem cavitation in the leaf and then rehydrated them for another 20 d. During that time, we monitored leaf shedding and senescence and measured the PLC of stems and leaves from different nodal positions. In the third experiment, we further studied stem embolism through the continuous monitoring of embolism with MRI during 10 d of dehydration.

The experimental material of the first two experiments consisted of own-rooted cv Chardonnay grapevine planted in 7-L pots. The plants were 3 years old and bore three to five current-year shoots, each ~1.5 m in length with approximately 20 nodes. In the third experiment, we used a 1-year-old cv Chardonnay grapevine grafted on SO4 rootstock in a 7.5-L pot, 2 months after bud burst, bearing four shoots and 80 leaves. Prior to the initiation of the experiments, all pots were irrigated daily to saturation.

Experiment 1: Dehydration through Cutting at the Root-Stem Junction

In experiment 1, four plants were cut at the soil-root interface and allowed to dehydrate for ~48 h at 25°C, 20% relative humidity, and 10 μmol photons m^{-2} s^{-1} incandescent light. Two leaves, one for g_s and one for embolism visualization, were monitored continuously. Both leaves were fully mature and had a similar nodal position (seventh to ninth leaves from the top) on two separate shoots. In addition, we followed the wilting of leaves during dehydration with a webcam (Logitech 920) programmed to acquire an image every 2 min. g_s was measured every 2 min for the first 6 to 8 h of the dehydration using a commercial gas-exchange system (LI-6400; LiCor). The measurements were taken at a constant light intensity (500 μmol m^{-2} s^{-1}) and CO_2 concentration (400 μmol mol^{-1}). Additionally, in four of these plants, the Ψ_l was measured every 1 to 5 h using a pressure chamber (Soil Moisture Equipment) to provide an ~0.2-MPa interval between Ψ_l measurements. Ψ_l values between measured time points were interpolated using the best-fit logarithmic model. For Ψ_l measurements, we used mature leaves that were at least three internodes distant from the imaged leaf.

Embolism spread was evaluated following the method of Brodribb et al. (2016b), in which embolism is detected by monitoring changes in light transmission through the xylem (Mayr et al., 2014; Ponomarenko et al., 2014). To provide either high spatial resolution or a large field of view, some leaves were imaged with a light microscope under 7.5× magnification (M80; Leica Microsystems) while others were imaged with a scanner (Epson perfection V800; Epson America). Leaves were imaged every 2 min (microscope) or 30 min (scanner) while drying for more than 40 h. The adaxial side of the leaf was fixed to the scanner/microscope surface using transparent double-sided tape, leaving the stomata uncovered. The leaf was illuminated from below to create an image of transmitted light, which was recorded by the scanner sensor or a digital camera (DFC290; Leica Microsystems). In the microscope, the imaged area of 17 × 10 mm encompassed all vein orders including the midrib; each image consisted of 1,920 × 1,080 pixels, resulting in a resolution of 8.8 μm per pixel (Fig. 9A). In the scanner, the imaged area consisted of half the leaf (including midrib) with a resolution of 21.3 μm per pixel.

To identify and quantify embolism events, image analysis was carried out using a custom algorithm executed in MATLAB (Mathworks). Consecutive images were subtracted to produce a set of difference images. In this series of subtracted images, white pixels represent any optical event: cavitation, instability of light conditions, and movements of the leaf, a trichome, or a bug. To separate the signal (cavitation event) from noise, the difference images were processed according to the following sequence: a brightness increase (25%), a median filtering using 3 × 3 neighboring pixels, a threshold adjustment (8%), and a second median filtering. The resulting images typically contain some degree of noise, normally originating from movements of trichomes or bugs, which therefore bear their shape. All images were examined carefully, and the remaining noise was removed manually. The degree of embolism was calculated as the cumulative number of embolized pixels normalized to the total number of embolized pixels throughout the dehydration. Finally, to visualize the dynamics of embolism spread through the leaf, events were colored on a continuous scale with respect to the time at which they appeared. To ensure that the imaging process itself did not result in cavitation, a fifth intact vine (i.e. still connected to its roots) in wet soil was imaged for 4 d without showing any sign of cavitation.

The light emitted by the gas-exchange system and the microscope could have resulted in higher transpiration rates and, thus, lower Ψ_l for the measured leaves relative to those exposed only to room light (Rockwell et al., 2014a). To evaluate the Ψ_l of these leaves, the dehydration experiment was repeated with four additional vines, with the difference that the experiment was stopped when g_s was equal to 20 mmol m^{-2} s^{-1} in order to evaluate Ψ_l using an isopiestic thermocouple psychrometer (Boyer, 1995). Leaf discs (2 cm^2) from the illuminated parts of the leaves in the gas-exchange system and microscope, as well as from two leaves exposed to room incandescent light, were excised directly into a psychrometer cup. To statistically compare the effect of the measurement conditions on the Ψ_l of the leaves, the Ψ_l differences between the illuminated leaves (microscope or gas-exchange system) and the leaves under room conditions were calculated. These Ψ_l differences were averaged and compared with each other (microscope versus gas-exchange system) using a two-tailed Student's t test, showing that when g_s was 20 mmol m^{-2} s^{-1}, leaves that were illuminated by the microscope or the gas-exchange system had, on average, 0.07 or 0.13 MPa lower Ψ_l ($n = 4$), respectively, than leaves exposed to room light. There was no significant difference in Ψ_l between the leaves in the gas-exchange system and the microscope ($P = 0.55$). Since Ψ_l differences were relatively small and are expected to be even smaller at the lower Ψ_l leading to cavitation (lower g_s), they were not considered. Therefore, g_s and embolism were plotted against the Ψ_l of leaves exposed to room light that could be slightly higher than the Ψ_l of measured leaves (for g_s or embolism).

Experiment 2: Dehydration of Intact Plants

In the second experiment, six vines were subjected to a dehydration-rehydration cycle lasting for 25 to 30 d. Additionally, three vines were maintained under constant well-watered conditions to serve as controls for the six experimental vines. Since imaging of all the repetitions could not be performed simultaneously, the experiment was repeated three times. In each repetition, three plants (two drying and a control plant) were monitored. The experiment was performed in a controlled environment (BDW80; Conviron) with day/night cycles of 14/10 h and temperatures of 25°C/20°C, respectively. Light intensity was 400 μmol m^{-2} s^{-1}, supplied from metal halide and halogen incandescent lamps, and relative humidity was between 50% and 75%. During the whole experiment, embolism spread in one leaf per plant was visualized continuously. Additionally, Ψ_l, g_s, and symptoms of leaf senescence were monitored frequently (at least 15 times per experiment). Ψ_l and g_s were measured at midday as described for the first experiment only on mature healthy leaves. The dehydration lasted for 5 to 10 d (depending on dehydration rate) and was stopped when the first leaf xylem embolism was observed. Because embolism appearance was evaluated once per day, rewatering occurred anywhere between 1 and 25 h after the first event was detected. From that day onward, the plants were irrigated to saturation daily. The experiment was terminated around 20 d after rehydration when a new emerging bud reached 2 cm in length. Buds appeared from the apical parts of the shoot.

Xylem embolism was evaluated similarly to the method described above for the first experiment. The upper part of the adaxial side of an intact leaf from the middle of the shoot was taped, using transparent double-sided tape, to the scanner surface (Epson perfection V800; Epson America; Fig. 9B). The abaxial part of the same leaf remained exposed to the atmosphere, allowing free gas exchange (grapevine is hypostomatous). Three times per day, in the beginning, middle, and end of the light period, the scanner lid was closed and an image was acquired. Aside from imaging time (8 min per scan taken three times per day), the scanner lid remained open to expose the leaf to ambient light and atmospheric conditions. Image analysis was performed as described above for the first experiment.

At the beginning of the dehydration cycle, leaves longer than 3 cm were counted. After the initiation of the experiment, the status of leaves was evaluated frequently to determine if they were damaged (at least 20% of the leaf with signs of necrosis), yellow (at least 20% with yellowing), or shed. A summary of these categories indicated the number of damaged leaves. To understand the relation between position along the shoot and the effects imposed by the drought, we assigned a nodal position index (between 0 and 1) to each leaf based on its actual nodal position (distance from the trunk in nodes) and the total number of nodes on the same shoot.

To compare the degree of embolism in leaves at low and high nodal positions, five more vines were dried in their pots for about 1 week. On the day when xylem embolism was detected in a leaf from the middle of the shoot, the plants were taken to the laboratory and eight shoots (from the five plants) were cut at their base under water. To evaluate the degree of embolism, we reversed the optical light transmission technique (Brodribb et al., 2016b) so that leaves were first imaged under native conditions (with potential embolism), pressurized with water at 150 kPa for 3 min to remove embolism, and then imaged again to see which vessels refilled. Throughout this process, the leaf was tightly taped to the scanner surface to minimize its movement. To avoid cavitation induced by cutting under tension (Wheeler et al., 2013; shown to occur in grape petioles by Hochberg et al., 2016b), the shoot base was maintained under water for 10 min to relax the xylem tension before harvesting the leaves. Then, the base of the petiole was cut under water, connected to tubing, and taped to the scanner.

Because pressurizing the leaf at 150 kPa resulted in substantial movement of the leaf, an alternative approach to evaluate the degree of embolism had to be taken. Instead of relying on whole-image subtraction (described for experiment 1) to produce difference images, we adopted a subsampling technique that is less vulnerable to movement of the leaf. Specifically, we measured the gray values in two polygons (~150 pixels each) per vein for six second-order veins located close to the leaf apex (detailed illustration in Fig. 9B). Only pixels from the center of the veins were selected. The same polygon was measured on both the before and after flushing images, and the relative change in gray values were calculated.

To validate the measurements conducted with the optical technique and provide metrics comparable to other studies, we quantified the degree of embolism in petioles from different nodal positions and the stem by hydraulic measurements. Two petioles per shoot (one from high and one from low nodal positions) were harvested under water from six tension-relaxed (10 min of relaxation) shoots and their PLC was measured with a Sperry-type apparatus (Sperry et al., 1988). With the same six shoots, one stem segment per shoot located at the center of the shoot was harvested and its PLC was determined. The downstream ends of the petiole or stem were connected to tubing, and the flow rates were monitored using a precision balance (CPA225D; Sartorius) connected with a personal computer. The flow passing through the stem/petiole section was generated by a 5-cm-high pressure head, with filtered (0.2 μm) 20 mmol of KCl solution used as the perfusion fluid. To reach the maximum conductance of a measured sample, petioles/stems were flushed for 3 min with a pressure head of 150 kPa, after which the flow direction was reversed and the sample was flushed again for another 3 min. To provide control values for both the relative change in gray values and PLC, six shoots from three well-watered vines were harvested and assessed as described above.

Experiment 3: MRI Dehydration

Some researchers argue that the xylem relaxation procedures could lead to xylem refilling and, thus, to underestimation of the native embolism degree (Trifilò et al., 2014; Knipfer et al., 2016). To assess the importance of such an effect in our analysis, we repeated the pot dehydration experiment (experiment 2) using MRI to monitor the degree of stem embolism in an intact vine. The imaged area was located 75 cm above the pot surface (45 cm from the graft) and 150 cm below the apex. The vine was left to dry in the imager under artificial light (300 μmol photons m^{-2} s^{-1}) until ~10% embolism was detected and then rehydrated to reveal the fate of its leaves. The 10% embolism was roughly estimated through comparison of the apparent number of total and embolized vessels. More accurate evaluations of embolism were performed only after the experiment was stopped, as described below.

All MRI work was done at the Institute for Bio- and Geosciences 2: Plant Sciences at the Forschungszentrum Jülich. The MRI scanner consisted of a Varian spectrometer, a 4KW RF amplifier, a set of 400A gradient amplifiers, and a custom-built 1.5 T superconducting magnet with a 50-cm vertical gap (Magnex Scientific). The magnet was fitted with an 800 mT/m biplanar gradient set (Tesla Engineering) and a 10-turn solenoidal RF coil. To create the coil, a Teflon former with a diameter of 15 mm (i.d.) was placed around the stem and a 0.5-mm copper wire was wound onto the former by hand and connected to a detachable tuning module.

Flow imaging was done using a pulsed field gradient-stimulated echo-multispin echo sequence, based on the sequence described by Windt et al. (2007). The following settings were used: field of view, 10 × 10 mm; slice thickness, 3 mm; matrix size, 128 × 64 pixels; pixel size, 78 × 156 μm; repetition time, 2.5 s (two averages); spectral width, 50 kHz; TE_1, 11.3 ms; and TE, 4.7 ms. Flow encoding used 32 Q steps, Δ 40 ms, δ 3 ms, and PFGmax 400 mT/m. While this sequence in principle would allow the acquisition of an echotrain with many echoes, in this study, only the first four echoes were used and averaged. The velocimetric data were processed as described by Scheenen et al. (2007) and Windt et al. (2006) to yield quantitative flow maps representing the amount of stationary water per pixel, the flow-conducting area per pixel, the average linear velocity of the flowing water, and the average volume flow per pixel.

Amplitude-T_2 imaging was done using a Carr Purcell Meiboom and Gill sequence with the following settings: field of view, 10 × 10 mm; slice thickness, 3 mm; matrix size, 256 × 256 pixels; pixel size, 39 × 39 μm; number of averages, eight; TE, 7.74 ms; number of echoes, 32; repetition time, 5 s; and spectral width, 50 kHz. The acquired data sets were fitted on a per pixel basis using a monoexponential decay function to yield quantitative maps of amplitude (water content per pixel) and T_2 (Edzes et al., 1998; van der Weerd et al., 2000).

The PLC derived from MRI images was calculated in two different ways. In the first, the maximum hydraulic conductance (k_{max}) was estimated as the sum of the theoretical hydraulic conductance of each vessel, based on its diameter (determined from the light microscopy cross-sectional image), and calculated according to Hagen-Poiseuille flow. The conductance loss (k_{loss}) was calculated on the basis of the diameters of the xylem vessels that turned black (gas filled) in the water content image. In the second approach, we overlaid the MRI water content image showing the embolism (Fig. 8A) with the MRI volume flow map from before embolism appearance to evaluate hydraulic conductance. k_{loss} was the sum of flow values of the pixels that turned black in the water content image, and k_{max} was the total flow based on the MRI volume flow map. PLC was calculated as $k_{loss}/k_{max} \times 100$.

Data and Statistical Analysis

g_s varied between the two experiments and between repetitions even before the treatments commenced, when all plants were under well-watered conditions. For a clear presentation and to allow comparison of the different experiments, all g_s data were normalized and are presented as percentage of before-treatment values.

In the second experiment, dehydration time for the six plants ranged from 5 to 10 d, probably because leaf area and dehydration rate were not identical across all plants and through the three different dehydration periods. For a clear presentation of the data, the dehydration period was stretched to the average dehydration period (7.16 d). For example, if it took only 5 d to reach embolism, every day was considered as 7.16/5. The degree of embolism or PLC was compared between apical and basal leaves using a paired-samples Student's t test, where samples from the same shoot were considered as pairs.

Supplemental Data

The following supplemental materials are available.

Supplemental Figure S1. Comparing embolism in different vein orders.

Supplemental Movie S1. Time lapse of embolism propagation in a grapevine leaf imaged with the microscope during 28 h after it was disconnected from its roots.

Supplemental Movie S2. Time lapse of embolism propagation in a grapevine leaf imaged with a scanner during 28 h after it was disconnected from its roots.

ACKNOWLEDGMENTS

We thank Dr. Kasia Zieminska for the cross-section preparation and CaviScan for technical support.

Received December 2, 2016; accepted March 25, 2017; published March 28, 2017.

LITERATURE CITED

Boyer JS (1995) Measuring the Water Status of Plants and Soils. Academic Press, San Diego

Boyer JS, Wong SC, Farquhar GD (1997) CO_2 and water vapor exchange across leaf cuticle (epidermis) at various water potentials. Plant Physiol **114:** 185–191

Brodersen CR, McElrone AJ, Choat B, Lee EF, Shackel KA, Matthews MA (2013) In vivo visualizations of drought-induced embolism spread in *Vitis vinifera*. Plant Physiol **161:** 1820–1829

Brodersen CR, McElrone AJ, Choat B, Matthews MA, Shackel KA (2010) The dynamics of embolism repair in xylem: in vivo visualizations using high-resolution computed tomography. Plant Physiol **154:** 1088–1095

Brodribb T, Holbrook N, Edwards E, Gutierrez M (2003) Relations between stomatal closure, leaf turgor and xylem vulnerability in eight tropical dry forest trees. Plant Cell Environ **26:** 443–450

Brodribb T, Holbrook NM (2003) Changes in leaf hydraulic conductance during leaf shedding in seasonally dry tropical forest. New Phytol **158:** 295–303

Brodribb TJ, Bienaimé D, Marmottant P (2016a) Revealing catastrophic failure of leaf networks under stress. Proc Natl Acad Sci USA **113:** 4865–4869

Brodribb TJ, Skelton RP, McAdam SA, Bienaimé D, Lucani CJ, Marmottant P (2016b) Visual quantification of embolism reveals leaf vulnerability to hydraulic failure. New Phytol **209:** 1403–1409

Charrier G, Torres-Ruiz JM, Badel E, Burlett R, Choat B, Cochard H, Delmas CE, Domec J, Jansen S, King A (2016) Evidence for hydraulic vulnerability segmentation and lack of xylem refilling under tension. Plant Physiol **172:** 1657–1668

Chatelet DS, Matthews MA, Rost TL (2006) Xylem structure and connectivity in grapevine (*Vitis vinifera*) shoots provides a passive mechanism for the spread of bacteria in grape plants. Ann Bot (Lond) **98:** 483–494

Choat B, Brodersen CR, McElrone AJ (2015) Synchrotron x-ray microtomography of xylem embolism in Sequoia sempervirens saplings during cycles of drought and recovery. New Phytol **205:** 1095–1105

Choat B, Drayton WM, Brodersen C, Matthews MA, Shackel KA, Wada H, McElrone AJ (2010) Measurement of vulnerability to water stress-induced cavitation in grapevine: a comparison of four techniques applied to a long-vesseled species. Plant Cell Environ **33:** 1502–1512

Christman MA, Sperry JS, Smith DD (2012) Rare pits, large vessels and extreme vulnerability to cavitation in a ring-porous tree species. New Phytol **193:** 713–720

Cochard H, Badel E, Herbette S, Delzon S, Choat B, Jansen S (2013) Methods for measuring plant vulnerability to cavitation: a critical review. J Exp Bot **64:** 4779–4791

Cochard H, Coll L, Le Roux X, Améglio T (2002) Unraveling the effects of plant hydraulics on stomatal closure during water stress in walnut. Plant Physiol **128:** 282–290

Cochard H, Delzon S (2013) Hydraulic failure and repair are not routine in trees. Ann Sci **70:** 659–661

Cochard H, Delzon S, Badel E (2015) X-ray microtomography (micro-CT): a reference technology for high-resolution quantification of xylem embolism in trees. Plant Cell Environ **38:** 201–206

Cuneo IF, Knipfer T, Brodersen CR, McElrone AJ (2016) Mechanical failure of fine root cortical cells initiates plant hydraulic decline during drought. Plant Physiol **172:** 1669–1678

Edzes HT, van Dusschoten D, Van As H (1998) Quantitative T_2 imaging of plant tissues by means of multi-echo MRI microscopy. Magn Reson Imaging **16:** 185–196

Herrera J, Bucchetti B, Sabbatini P, Comuzzo P, Zulini L, Vecchione A, Peterlunger E, Castellarin S (2015) Effect of water deficit and severe shoot trimming on the composition of *Vitis vinifera* L. Merlot grapes and wines. Aust J Grape Wine Res **21:** 254–265

Hochberg U, Albuquerque C, Rachmilevitch S, Cochard H, David-Schwartz R, Brodersen CR, McElrone A, Windt CW (2016a) Grapevine petioles are more sensitive to drought induced embolism than stems: evidence from in vivo MRI and microcomputed tomography observations of hydraulic vulnerability segmentation. Plant Cell Environ **39:** 1886–1894

Hochberg U, Herrera JC, Cochard H, Badel E (2016b) Short-time xylem relaxation results in reliable quantification of embolism in grapevine petioles and sheds new light on their hydraulic strategy. Tree Physiol **36:** 748–755

Hochberg U, Herrera JC, Degu A, Castellarin SD, Peterlunger E, Alberti G, Lazarovitch N (2017) Evaporative demand determines the relative transpirational sensitivity of deficit-irrigated grapevines. Irrig Sci **35:** 1–9

Holbrook NM, Ahrens ET, Burns MJ, Zwieniecki MA (2001) In vivo observation of cavitation and embolism repair using magnetic resonance imaging. Plant Physiol **126:** 27–31

Jacobsen AL, Rodriguez-Zaccaro FD, Lee TF, Valdovinos J, Toschi HS, Martinez JA, Pratt RB (2015) Grapevine xylem development, architecture, and function. *In* Functional and Ecological Xylem Anatomy. Springer, Cham, Switzerland, pp 133–162

Klein T, Cohen S, Paudel I, Preisler Y, Rotenberg E, Yakir D (2016) Diurnal dynamics of water transport, storage and hydraulic conductivity in pine trees under seasonal drought. iForest Biogeosciences and Forestry **9:** e1–e10

Knipfer T, Cuneo IF, Brodersen CR, McElrone AJ (2016) In situ visualization of the dynamics in xylem embolism formation and removal in the absence of root pressure: a study on excised grapevine stems. Plant Physiol **171:** 1024–1036

Knipfer T, Eustis A, Brodersen C, Walker AM, McElrone AJ (2015) Grapevine species from varied native habitats exhibit differences in embolism formation/repair associated with leaf gas exchange and root pressure. Plant Cell Environ **38:** 1503–1513

Lens F, Tixier A, Cochard H, Sperry JS, Jansen S, Herbette S (2013) Embolism resistance as a key mechanism to understand adaptive plant strategies. Curr Opin Plant Biol **16:** 287–292

Lovisolo C, Perrone I, Hartung W, Schubert A (2008) An abscisic acid-related reduced transpiration promotes gradual embolism repair when grapevines are rehydrated after drought. New Phytol **180:** 642–651

Lovisolo C, Schubert A (1998) Effects of water stress on vessel size and xylem hydraulic conductivity in Vitis vinifera L. J Exp Bot **49:** 693–700

Mayr S, Kartusch B, Kikuta S (2014) Evidence for air-seeding: watching the formation of embolism in conifer xylem. J Plant Hydraul **1:** e0004

McCulloh KA, Meinzer FC (2015) Further evidence that some plants can lose and regain hydraulic function daily. Tree Physiol **35:** 691–693

McElrone AJ, Brodersen CR, Alsina MM, Drayton WM, Matthews MA, Shackel KA, Wada H, Zufferey V, Choat B (2012) Centrifuge technique consistently overestimates vulnerability to water stress-induced cavitation in grapevines as confirmed with high-resolution computed tomography. New Phytol **196:** 661–665

Mott K, Franks P (2001) The role of epidermal turgor in stomatal interactions following a local perturbation in humidity. Plant Cell Environ **24:** 657–662

Nardini A, Salleo S (2000) Limitation of stomatal conductance by hydraulic traits: sensing or preventing xylem cavitation? Trees (Berl) **15:** 14–24

Pivovaroff AL, Burlett R, Lavigne B, Cochard H, Santiago LS, Delzon S (2016) Testing the 'microbubble effect' using the Cavitron technique to measure xylem water extraction curves. AoB Plants **8:** plw011

Pockman WT, Sperry JS, O'Leary JW (1995) Sustained and significant negative water pressure in xylem. Nature **378:** 715–716

Ponomarenko A, Vincent O, Pietriga A, Cochard H, Badel É, Marmottant P (2014) Ultrasonic emissions reveal individual cavitation bubbles in water-stressed wood. J R Soc Interface **11:** 11

Rockwell FE, Holbrook NM, Stroock AD (2014a) The competition between liquid and vapor transport in transpiring leaves. Plant Physiol **164:** 1741–1758

Rockwell FE, Wheeler JK, Holbrook NM (2014b) Cavitation and its discontents: opportunities for resolving current controversies. Plant Physiol **164:** 1649–1660

Scheenen TW, Vergeldt FJ, Heemskerk AM, Van As H (2007) Intact plant magnetic resonance imaging to study dynamics in long-distance sap flow and flow-conducting surface area. Plant Physiol **144:** 1157–1165

Schultz HR (2003) Differences in hydraulic architecture account for near isohydric and anisohydric behaviours of two field-grown Vitis vinifera L. cultivars during drought. Plant Cell Environ **26:** 1393–1405

Schultz HR, Matthews MA (1988) Resistance to water transport in shoots of *Vitis vinifera* L.: relation to growth at low water potential. Plant Physiol **88:** 718–724

Scoffoni C, Albuquerque C, Brodersen CR, Townes SV, John GP, Cochard H, Buckley TN, McElrone AJ, Sack L (2017) Leaf vein xylem conduit diameter influences susceptibility to embolism and hydraulic decline. New Phytol **213:** 1076–1092

Sperry J, Donnelly J, Tyree M (1988) A method for measuring hydraulic conductivity and embolism in xylem. Plant Cell Environ **11:** 35–40

Torres-Ruiz JM, Cochard H, Mayr S, Beikircher B, Diaz-Espejo A, Rodriguez-Dominguez CM, Badel E, Fernández JE (2014) Vulnerability to cavitation in *Olea europaea* current-year shoots: further evidence of an open-vessel artifact associated with centrifuge and air-injection techniques. Physiol Plant **152:** 465–474

Torres-Ruiz JM, Jansen S, Choat B, McElrone AJ, Cochard H, Brodribb TJ, Badel E, Burlett R, Bouche PS, Brodersen CR, et al (2015) Direct x-ray microtomography observation confirms the induction of embolism upon xylem cutting under tension. Plant Physiol **167:** 40–43

Trifilò P, Nardini A, Lo Gullo MA, Barbera PM, Savi T, Raimondo F (2015) Diurnal changes in embolism rate in nine dry forest trees: relationships with species-specific xylem vulnerability, hydraulic strategy and wood traits. Tree Physiol **35:** 694–705

Trifilò P, Raimondo F, Lo Gullo MA, Barbera PM, Salleo S, Nardini A (2014) Relax and refill: xylem rehydration prior to hydraulic measurements favours embolism repair in stems and generates artificially low PLC values. Plant Cell Environ **37:** 2491–2499

Tyree MT, Sperry JS (1988) Do woody plants operate near the point of catastrophic xylem dysfunction caused by dynamic water stress? Answers from a model. Plant Physiol **88:** 574–580

Van den Honert T (1948) Water transport in plants as a catenary process. Discuss Faraday Soc **3:** 146–153

van der Weerd L, Vergeldt FJ, Adrie de Jager P, Van As H (2000) Evaluation of algorithms for analysis of NMR relaxation decay curves. Magn Reson Imaging **18:** 1151–1158

Venturas MD, Rodriguez-Zaccaro FD, Percolla MI, Crous CJ, Jacobsen AL, Pratt RB (2016) Single vessel air injection estimates of xylem resistance to cavitation are affected by vessel network characteristics and sample length. Tree Physiol **36:** 1247–1259

Wheeler JK, Huggett BA, Tofte AN, Rockwell FE, Holbrook NM (2013) Cutting xylem under tension or supersaturated with gas can generate PLC and the appearance of rapid recovery from embolism. Plant Cell Environ **36:** 1938–1949

Windt CW, Vergeldt FJ, de Jager PA, van As H (2006) MRI of long-distance water transport: a comparison of the phloem and xylem flow characteristics and dynamics in poplar, castor bean, tomato and tobacco. Plant Cell Environ **29:** 1715–1729

Windt CW, Vergeldt FJ, Van As H (2007) Correlated displacement-T_2 MRI by means of a pulsed field gradient-multi spin echo method. J Magn Reson **185:** 230–239

Wolfe BT, Sperry JS, Kursar TA (2016) Does leaf shedding protect stems from cavitation during seasonal droughts? A test of the hydraulic fuse hypothesis. New Phytol **212:** 1007–1018

Zhang YJ, Rockwell FE, Graham AC, Alexander T, Holbrook NM (2016) Reversible leaf xylem collapse: a potential "circuit breaker" against cavitation. Plant Physiol **172:** 2261–2274

Zimmermann MH (1983) The hydraulic architecture of plants. *In* Xylem Structure and the Ascent of Sap. Springer, New York, pp 66–82

Zufferey V, Cochard H, Ameglio T, Spring JL, Viret O (2011) Diurnal cycles of embolism formation and repair in petioles of grapevine (*Vitis vinifera* cv. Chasselas). J Exp Bot **62:** 3885–3894